arXiv:1501.06453v2 [physics.atom-ph] 2 Feb 2015

Quantum Algorithmic Readout in Multi-Ion Clocks

M. Schulte,[1] N. Lörch,[1] I. D. Leroux,[2] P. O. Schmidt,[2,3] and K. Hammerer[1]

[1] *Institute for Theoretical Physics and Institute for Gravitational Physics (Albert-Einstein-Institute), Leibniz University Hannover, Callinstrasse 38, 30167 Hannover, Germany*

[2] *QUEST Institut, Physikalisch-Technische Bundesanstalt, 38116 Braunschweig, Germany*

[3] *Institute for Quantum Optics, Leibniz University Hannover, Welfengarten 1, 30167 Hannover, Germany*

(Dated: February 3, 2015)

Optical clocks based on ensembles of trapped ions promise record frequency accuracy with good short-term stability. Most suitable ion species lack closed transitions for state detection, so the clock signal must be read out indirectly by transferring the quantum state of the clock ions to co-trapped logic ions using quantum logic operations. Existing methods of quantum logic readout require a linear overhead in either time or the number of logic ions. Here we describe a quantum algorithmic readout whose overhead scales logarithmically with the number of clock ions in both of these respects. We show that the readout can be performed with a single application of a multi-species quantum gate, which we describe in detail for a crystal of Al^+ and Ca^+ ions.

Tremendous progress has recently been made in optical frequency metrology [1, 2]. Optical clocks now reach fractional frequency inaccuracies and instabilities in the 10^{-18} regime [3–8], outperforming Cs fountain clocks by two orders of magnitude and vying to serve as a new definition of the SI second [9, 10]. Among the promising candidates for such a redefinition are ion-based frequency standards featuring very small systematic frequency shifts. However, the poor signal-to-noise ratio of single-ion systems entails averaging times of many weeks to reach a fractional uncertainty of 10^{-18} [11, 12]. Clocks based on strings of ions confined in a linear trap promise to overcome this limitation [13, 14]. Due to unavoidable electric field gradients in such a trap, suitable clock ion species may have only negligible electric quadrupole moments to avoid systematic frequency shifts [15]. This requirement is met by group 13 ion species featuring a ${}^1S_0 \leftrightarrow {}^3P_0$ transition [16], as well as some highly-charged ions [17–20]. Most of these candidates (with the notable exception of In^+) lack a suitable transition for laser cooling and state detection, so that quantum logic spectroscopy (QLS) [21] is required for readout. In QLS, the internal state of the clock ion is transferred by a series of laser pulses onto a logic ion, where it can be efficiently detected. However, existing methods for quantum logic readout require a large overhead in either time or logic ions when an ensemble of clock ions is used.

Here, we suggest using a quantum algorithm originally developed in the context of entanglement concentration for a quantum non-demolition (QND) measurement of the clock signal. The number of logic ions and gate operations required both scale as the logarithm of the number of clock ions. We show that the algorithm can be implemented efficiently using the multi-ion Mølmer-Sørensen gate [22–25], a well-established tool for quantum control of ion crystals [26, 27]. We demonstrate the feasibility of such gates in multi-species crystals, for instance with 3 Al^+ and 2 Ca^+ ions. The QND readout we propose opens up rich perspectives for more complex clock protocols.

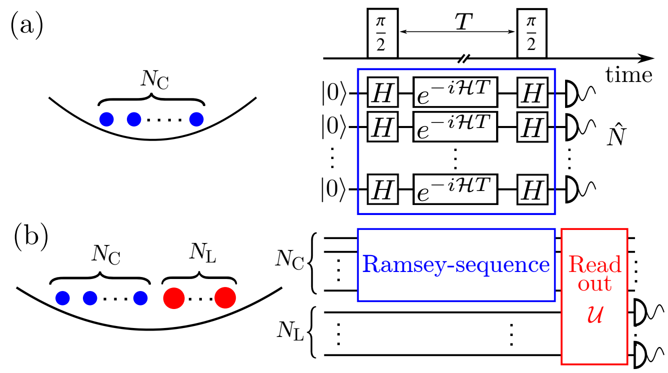

FIG. 1. (a) In an atomic clock based on N_C trapped ions the frequency of a laser is locked to an atomic transition of frequency ω_0 *e.g.* in a Ramsey sequence of two $\pi/2$-pulses (Hadamard gates H) enclosing a free evolution time T (with Hamiltonian $\mathcal{H}$). Measurement of the number $\hat{N}$ of clock ions in $|1\rangle$ yields an error signal for the deviation of the laser from resonance. (b) For ion species lacking the cycling transition needed for direct state detection, a quantum algorithmic readout can be used to map $\hat{N}$ onto N_L co-trapped logic ions whose state can be detected efficiently.

Working principle of ion clocks with direct readout—We consider a string of N_C clock ions with a narrow-band optical transition of frequency ω_0 between two internal states $|0\rangle$ and $|1\rangle$ which provides the frequency reference for the clock. The goal is to stabilize to this transition frequency ω_0 a laser field of frequency ω. To this end, pulses of light from the laser drive the clock ions, transferring them from $|0\rangle$ to the excited state $|1\rangle$ with a frequency-dependent probability. In the simplest schemes, such as Rabi and Ramsey interrogation, this probability is independent for each ion. The clock readout then consists in measuring the number of excited ions $\hat{N} = \sum_{i=1}^{N_C} |1\rangle_i\langle 1|$ and using it to infer the excitation probability and thence the frequency offset $\Delta = \omega - \omega_0$, which can then be corrected. For definiteness we illustrate our proposed scheme with Ramsey interrogation (cf. Fig. 2a), but note

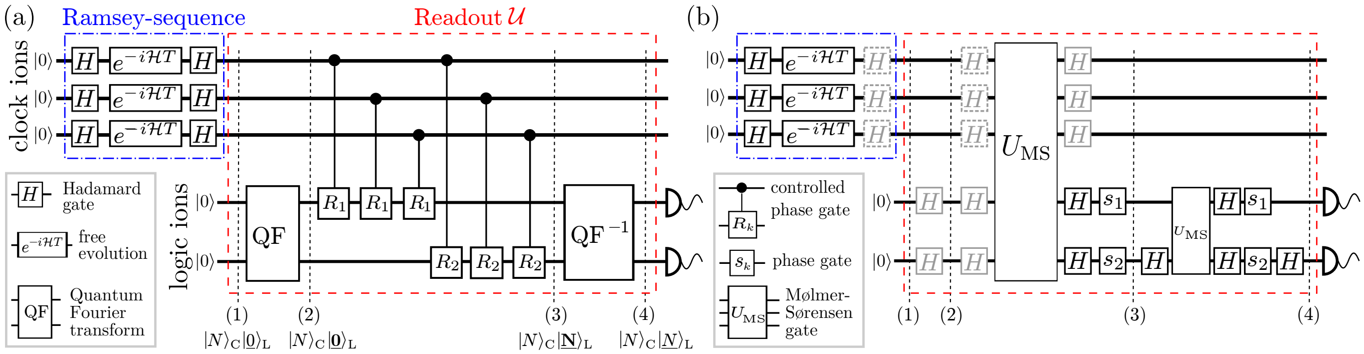

FIG. 2. Quantum algorithmic readout illustrated for $N_{\rm C}=3$ clock and $N_{\rm L}=2$ logic ions: after a Ramsey sequency (blue, dash-dotted box) the clock ions are in a superposition of states $|N\rangle_{\rm C}$ where $N\in[0,N_{\rm C}]$ is the number of ions in excited states $|1\rangle$ (their Hamming weight). A quantum algorithmic readout $\mathcal{U}$ (red, dashed box) maps N in binary representation onto a number $N_{\rm L}=\lceil\log_2(N_{\rm C}+1)\rceil$ of logic ions. Detection of the logic ions in the $\{|0\rangle,|1\rangle\}$-basis provides the number N. (a) Quantum algorithm for the indirect measurement of the Hamming weight, taken from [28, 29]: (1) Logic ions are initialized in $|\underline{0}\rangle_{\rm L}=|00\rangle_{\rm L}$ (states $|\underline{N}\rangle_{\rm L}$ denote the binary representation of N). (2) The state is quantum Fourier transformed into $|\underline{\mathbf{0}}\rangle_{\rm L}$. (3) Controlled-phase gates rotate the state in Fourier space to $|\underline{\mathbf{N}}\rangle_{\rm L}$ for a state $|N\rangle_{\rm C}$ of clock ions. (4) An inverse Fourier transform yields the state $|\underline{N}\rangle_{\rm L}$ of logic ions. (b) The same algorithm decomposed in terms of multi-ion Mølmer-Sørensen (MS). The Hadamard gates shown in grey need not be executed. Removing Hadamard gates displayed with dashed boxes merges the algorithmic readout with the Ramsey sequence, and requires the laser fields in the MS gates to be phase coherent with the Hadamard gates in the Ramsey sequence. Explicit, general forms of all gates are given in the Appendix.

that arbitrary clock protocols involving entangled states and correlations between ion excitation probabilities can always be designed to yield $N_{\rm C}+1$ measurement eigenvalues corresponding to the different possible numbers of excited ions [30]. A method to measure $\hat{N}$ can thus be used to read out any $N_{\rm C}$-ion clock.

As explained above, a direct measurement of the excited state population $\hat{N}$ is impractical for many interesting species of clock ion. Instead, one can map $\hat{N}$ onto an ensemble of $N_{\rm L}$ co-trapped logic ions which can be detected efficiently, as shown in Fig. 1b. In direct extension of established readout techniques based on quantum logic [21, 31] one could use as many logic ions as clock ions ($N_{\rm L}=N_{\rm C}$), performing successive quantum gate operations to transfer the state of each clock ion to the corresponding logic ion. Alternatively, one could use a single logic ion, transfer the state of each clock ion sequentially to the logic ion, and measure it there. This imposes a long readout time as the ion crystal must be cooled between each measurement and subsequent state swap operation. Both strategies have prohibitive overhead in additional ions or number of gate operations and readout time. The last is crucial because time spent on readout adds to the clock cycle's dead time and thus, through the Dick effect, to the clock instability [32, 33].

Quantum algorithmic readout— From the perspective of Quantum Information Theory the quantity of interest — the number of clock ions in state $|1\rangle$ — is the *Hamming weight* of the string of $N_{\rm C}$ quantum bits (a number with $N_{\rm C}+1$ possible values between 0 and $N_{\rm C}$). In the context of entanglement concentration protocols a quantum algorithm has been developed for the indirect determination of the Hamming weight of a quantum bit string [28, 29], cf. Fig. 2a. The algorithm uses an ancillary string of $N_{\rm L}=\lceil\log_2(N_{\rm C}+1)\rceil$ quantum bits on which the Hamming weight of the $N_{\rm C}$ primary quantum bits is stored in binary representation. Thus the necessary number $N_{\rm L}$ of logic ions (ancillary quantum bits) scales logarithmically with the number of clock ions. Suitable combinations of clock and logic ion numbers $(N_{\rm C},N_{\rm L})$ are, for example, $(3,2)$ and $(7,3)$. Given $N_{\rm C}$ quantum bits (clock ions) in a state $|N\rangle_{\rm C}$ with Hamming weight N and $N_{\rm L}$ ancillary bits (logic ions) initialized in $|00\ldots0\rangle_{\rm L}$, the algorithm effects a unitary transformation $\mathcal{U}$ such that $\mathcal{U}|N\rangle_{\rm C}|00\ldots0\rangle_{\rm L}=|N\rangle_{\rm C}|i_1i_2\ldots i_{N_{\rm L}}\rangle_{\rm L}$ where $|N\rangle_{\rm C}$ denotes the normalized, symmetric superpostion of N clock ions in $|1\rangle$ and all others in $|0\rangle$ [34] and the bit string $i_1i_2\ldots i_{N_{\rm L}}$ ($i_n=0,1$) in the state of the logic ions gives the binary representation of the Hamming weight of the state of clock ions, $N=\sum_{n=1}^{N_{\rm L}}2^{n-1}i_n$. We will denote by $|\underline{N}\rangle_L=|i_1i_2\ldots i_{N_{\rm L}}\rangle_{\rm L}$ the state of logic ions representing N. The state of the clock ions after one clock cycle is a superposition $|\psi(\Delta)\rangle_{\rm C}=\sum_{N=0}^{N_{\rm C}}c_N(\Delta)|N\rangle_{\rm C}$ where the dependence of the amplitudes $c_N(\Delta)$ on the detuning carries the clock signal. Application of the readout algorithm generates an entangled state of clock and logic ions

$$|\Psi(\Delta)\rangle=\mathcal{U}|\psi(\Delta)\rangle_{\rm C}|\underline{0}\rangle_{\rm L}=\sum_{N=0}^{N_{\rm C}}c_N(\Delta)|N\rangle_{\rm C}|\underline{N}\rangle_L.$$

From a measurement in the $\{|0\rangle,|1\rangle\}$-basis of each logic ion one can extract the observable corresponding to the *estimated* Hamming weight of the clock ions $\hat{N}_{\rm est}=\sum_{n=1}^{N_{\rm L}}2^{n-1}|1\rangle_n\langle1|=\sum_{N=0}^{N_{\rm C}}N|\underline{N}\rangle_{\rm L}\langle\underline{N}|$. In a perfect implementation measurement of $\hat{N}_{\mathrm{est}}$ on the logic ions exhibits *exactly* the same statistics as measuring $\hat{N}$ on the clock ions directly. In particular, the error signal can be extracted from $N(\Delta) = \langle\Psi(\Delta)|\hat{N}_{\mathrm{est}}|\Psi(\Delta)\rangle$ and used to correct ω exactly as in a direct readout.

Implementation based on Mølmer-Sørensen gates— Following [28, 29], the operation $\mathcal{U}$ can be implemented by a sequence of quantum Fourier transforms and controlled-phase gates as shown in Fig. 2a. This requires a number of gates linear in N_{C}, so provides little advantage over the complete state swap mentioned above (apart from the reduction in the number of logic ions). Fortunately, the algorithm can be decomposed much more efficiently using the tools of quantum control available in linear ion traps. Many experiments on quantum computations and simulations [26, 27] exploit multi-ion Mølmer-Sørensen (MS) gates [22–24], which are unitary transformations $U_{\mathrm{MS}} = \exp(-iS^2)$ where

$$S = \sum_{\alpha=\mathrm{L,C}} \sum_{i=1}^{N_\alpha} d_{\alpha i}\big(\sigma^x_{\alpha i}\cos\phi_{\alpha i} + \sigma^y_{\alpha i}\sin\phi_{\alpha i}\big), \qquad (1)$$

and $\sigma^{x(y)}_{\alpha i}$ denotes a Pauli $x(y)$-operator for the i-th clock or logic ion for, respectively, $\alpha = \mathrm{L,C}$ ($i = 1,\ldots,N_\alpha$). A MS gate involves driving the ions simultaneously with bichromatic laser fields at frequencies $\omega_0 \pm (\nu+\delta)$ for a time t where ν denotes the frequency of one of the collective modes of vibration in the ion crystal, and $\delta > 0$ is the detuning from the respective sideband transition, cf. [25] and Appendix. The coefficients in S are given by

$$d_{\alpha i} = \Omega_{\alpha i}\eta_{\alpha i}\sqrt{t/\delta} \qquad (2)$$

where $\Omega_{\alpha i}$ is the Rabi frequency of the laser and $\eta_{\alpha i}$ is a Lamb-Dicke factor. Off-resonant driving requires $|\Omega_{\alpha i}\eta_{\alpha i}/\delta| \ll 1$. The angles $\phi_{\alpha i}$ in (1) are set by the phase of the laser fields. Here, we assume transverse illumination of the crystal, driving sideband transitions to a collective mode of radial vibration, so that the laser field at each ion can be adjusted separately. We consider the feasibility of tailoring suitable values of $\Omega_{\alpha i}$ and $\phi_{\alpha i}$ below, with a concrete case study of a multi-species MS gate.

A decomposition of the desired transformation $\mathcal{U}$ in terms of multi-ion MS gates and single ion rotations is shown in Fig. 2b. Remarkably, only a *single* two-species MS gate is required. The inverse Fourier transform on the string of logic ions involves $N_{\mathrm{L}} - 1$ single-species MS gates such that the total number N_{L} of multiqubit gates grows *logarithmically* with the number of clock ions N_{C} (cf. Appendix). What is more, the clock ions are involved only *once* in the first MS gate. In contrast, a readout relying on a state swap between N_{C} clock and $N_{\mathrm{L}} = N_{\mathrm{C}}$ logic ions requires N_{C} gate operations each of which acts on a pair of one clock and one logic ion. Compared to this, the readout strategy introduced here offers a considerable advantage even for the small ion numbers $(N_{\mathrm{C}}, N_{\mathrm{L}}) = (3,2)$ and $(7,3)$ most relevant to experiments.

In the first MS gate of Fig. 2b the laser phases must be chosen as $\phi_{\alpha i} = 0$ or π, such that S involves σ^x-operators only, and the coefficients $d_{\alpha i}$ in Eq. (1) must satisfy

$$d_{\mathrm{C}i}d_{\mathrm{L}j}e^{i(\phi_{\mathrm{C}i}+\phi_{\mathrm{L}i})} = -\pi\,2^{-(j+2)}, \qquad (3)$$

$$d_{\mathrm{L}j}d_{\mathrm{L}k} = \pi\,n_{jk} \qquad (j \neq k), \qquad (4)$$

where $i = 1,\ldots,N_{\mathrm{C}}$, $j,k = 1,\ldots,N_{\mathrm{L}}$ and n_{jk} are integers. Condition (3) ensures that the MS gate executes the controlled phase gates between logic and clock ions as shown in Fig. 2a. Condition (4) guarantees that the logic ions effectively do not interact with each other during the MS gate operation. The solution that minimizes the size of the largest coefficient is

$$|d_{\mathrm{L}j}| = \sqrt{\pi}\,2^{N_{\mathrm{L}}-1-j}, \qquad |d_{\mathrm{C}i}| = \sqrt{\pi}\,2^{-(N_{\mathrm{L}}+1)}. \qquad (5)$$

The signs of $d_{\alpha i}$ are determined (through the Lamb-Dicke factors $\eta_{\alpha i}$) by the sense of each ion's motion in the normal mode used in the MS gate. For a given normal mode the laser phases $\phi_{\alpha i}$ must be chosen to yield the correct sign in condition (3). The MS gates in the subsequent inverse Fourier transform concern logic ions only ($d_{\mathrm{C}i} = 0$). The required values of $d_{\mathrm{L}i}$ are similar to those in the first MS gate, and at most $\sqrt{2\pi}\cdot 2^{N_{\mathrm{L}}-3}$. The explicit expressions are given in the Appendix.

In the remainder of this article we discuss in more detail the realization of multi-species MS gates for the concrete case of Al^+ and Ca^+ as clock and logic ions respectively. The main requirement for an efficient MS gate is a well-resolved normal mode of vibration that involves both clock and logic ions, so we start by finding the normal mode spectrum of the two-species crystal. We assume the ions are held in a linear RF Paul trap with soft confinement along the crystal axis (z-axis) at vibration frequency ν^{L}_z (for logic ions, as a reference), and much tighter confinement in the transverse directions. We also assume that transverse oscillations are effectively restricted to one direction (x-axis) by stiff confinement in the other. It is important to note that the two species of ions experience different radial potentials because the pseudopotential generated by the radial AC fields in a Paul trap is mass-dependent. As a result, lighter ions feel a tighter transverse potential. The corresponding trap frequencies of clock and logic ions are denoted by ν^{C}_x and ν^{L}_x, where $\nu^{\mathrm{L}}_x < \nu^{\mathrm{C}}_x$ since $m_{\mathrm{Al}}/m_{\mathrm{Ca}} = 27/40$. Let $a = \nu^{\mathrm{L}}_x/\nu^{\mathrm{L}}_z$ be the asymmetry parameter between the axial and the smaller of the two radial frequencies. Taking into account the Coulomb repulsion and assuming a particular ordering of ions along the axis, we determine the average position of ions and the normal modes of vibrations following [35–37], see also the Appendix. The generic result is that for large asymmetry parameter a

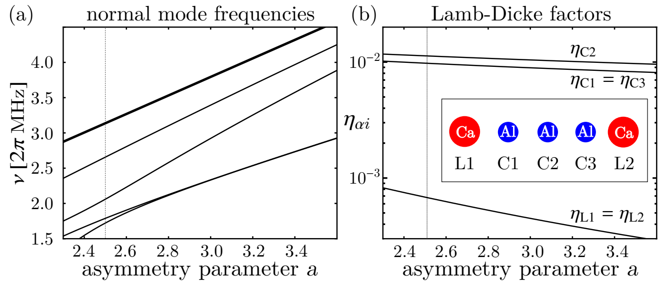

FIG. 3. (a) Normal mode frequencies of transverse vibration for a crystal of $N_C = 3$ Al^+ clock ions between $N_L = 2$ Ca^+ logic ions (see b, inset) versus asymmetry parameter $a = \nu_x^L/\nu_z^L$ (ratio of transverse to axial trap frequencies for logic ions, $\nu_z^L = 2\pi\,874\,\mathrm{kHz}$). (b) Lamb-Dicke factors η_{Ci} and η_{Lj} of, respectively, the three clock and two logic ions for the normal mode of highest frequency (thick line in (a)). For large asymmetry parameter transverse motions of clock and logic ions decouple due to the mass-dependent transverse confinement. The dotted line in (a) and (b) marks the case studied in the text.

the $N_L + N_C$ normal modes split into two groups involving either the N_L logic or the N_C clock ions. To have truly collective normal modes involving both species of ions (as required for the MS gate) the asymmetry must be kept moderate. However, below a critical value of a the normal modes become unstable and the crystal changes to a zig-zag configuration [35–37].

In Fig. 3a we show the spectrum of the transverse normal modes for the case of $(N_C, N_L) = (3, 2)$ in the ordering shown in the inset of Fig. 3b. For moderate trap asymmetry the highest-lying mode is sufficiently collective while exhibiting a substantial gap $\Delta\nu$ to the neighboring mode. This gap sets the time-scale for the gate operation: the detuning in the MS gate must be small enough ($\delta \ll \Delta\nu$) to avoid coupling to the wrong mode, and the Rabi frequencies must obey $|\Omega_{\alpha i}\eta_{\alpha i}| \ll \delta$. Finally, the $\Omega_{\alpha i}$ and the gate duration t in Eq. (2) must be chosen to satisfy the conditions in Eqs. (5) for the MS gate. For an axial trap frequency of $2\pi\,874\,\mathrm{kHz}$ and an asymmetry parameter $a = 2.5$ the highest-lying transverse mode has a frequency $\nu = 2\pi\,3.14\,\mathrm{MHz}$ and the gap to the next mode is $\Delta\nu = 2\pi\,480\,\mathrm{kHz}$. Assuming all laser beams are aligned with the x-axis, the corresponding Lamb-Dicke parameters are $\eta_{Li} = 0.007$ for both logic ions and $\eta_{C1} = \eta_{C3} = 0.097$, $\eta_{C2} = 0.113$ for the clock ions, see Fig. 3b. For a detuning $\delta = 2\pi\,24\,\mathrm{kHz}$ and a gate duration $t = 1\,\mathrm{ms}$ we choose the Rabi frequencies $(\Omega_{L1}, \Omega_{L2}) = 2\pi\,(500, 250)\,\mathrm{kHz}$ and $(\Omega_{C1}, \Omega_{C2}, \Omega_{C3}) = 2\pi\,(4.51, 3.87, 4.51)\,\mathrm{kHz}$ for logic and clock ions, respectively, satisfying Eq. (5). In this example $\delta/\Delta\nu$ is 5% and the largest of the ratios $|\Omega_{\alpha i}\eta_{\alpha i}|/\delta$ is 15%. Note that the carrier transition is driven off-resonantly with a Rabi frequency to detuning ratio of $\Omega_{\alpha i}/\nu$ which is also on the order of 15%. However, the associated AC Stark shifts cancel due to the bichromatic, red- and blue-detuned drive.

The 1 ms gate duration is short enough compared to the 1.17 s $D_{5/2}$ state lifetime in Ca^+ that readout errors due to spontaneous emission will be on the per mill level, as confirmed by a full solution of a master equation, see also Appendix. The Rabi frequencies required in the present example can be tailored by implementing the gate with a tightly focused TEM_{10} laser beam, such that each ion is located at a position in the transverse intensity profile corresponding to the Rabi frequency given above.

The more complex spatial structure of Rabi frequencies needed in a longer string of ions can be engineered with spatial light modulators [38] or multi-channel acousto-optical modulators. Combined with the freedom to permute clock and logic ions and to choose different solutions to Eqs. (3)-(4) we expect experimentally feasible implementations for more than 15 clock and 4 logic ions. With more ions, the narrower spacing of collective modes may require active compensation of off-resonant couplings to spectator modes.

Note that the quantum algorithmic readout suggested here performs a QND measurement of the Hamming weight of clock ions. This may allow more complex clock protocols using repeated readouts of (sub)ensembles of ions or preparation of the clock ions in Dicke states for nonclassical frequency metrology.

Acknowledgements— We acknowledge support from DFG through QUEST. I.D.L. acknowledges support from the Alexander von Humboldt Foundation. This work was supported by the European Metrology Research Programme (EMRP) in project SIB04. The EMRP is jointly funded by the EMRP participating countries within EURAMET and the European Union.

[1] N. Poli, C. W. Oates, P. Gill, and G. M. Tino, Riv. Nuovo Cimento **36**, 555 (2013).
[2] A. D. Ludlow, M. M. Boyd, J. Ye, E. Peik, and P. Schmidt, arXiv:1407.3493v1 (2014).
[3] T. Rosenband, D. B. Hume, P. O. Schmidt, C. W. Chou, A. Brusch, L. Lorini, W. H. Oskay, R. E. Drullinger, T. M. Fortier, J. E. Stalnaker, S. a. Diddams, W. C. Swann, N. R. Newbury, W. M. Itano, D. J. Wineland, and J. C. Bergquist, Science **319**, 1808 (2008).
[4] C. W. Chou, D. B. Hume, J. C. J. Koelemeij, D. J. Wineland, and T. Rosenband, Phys. Rev. Lett. **104**, 070802 (2010).
[5] C. W. Chou, D. B. Hume, M. J. Thorpe, D. J. Wineland, and T. Rosenband, Phys. Rev. Lett. **106**, 160801 (2011).
[6] N. Hinkley, J. A. Sherman, N. B. Phillips, M. Schioppo, N. D. Lemke, K. Beloy, M. Pizzocaro, C. W. Oates, and A. D. Ludlow, Science **341**, 1215 (2013).
[7] B. J. Bloom, T. L. Nicholson, J. R. Williams, S. L. Campbell, M. Bishof, X. Zhang, W. Zhang, S. L. Bromley, and J. Ye, Nature **506**, 71 (2014).
[8] I. Ushijima, M. Takamoto, M. Das, T. Ohkubo, and H. Katori, arXiv:1405.4071 [physics] (2014).
[9] P. Gill, Philos. T. R. Soc. A **369**, 4109 (2011).

[10] F. Riehle, arXiv:1501.02068 [physics] (2015), arXiv: 1501.02068.

[11] G. Santarelli, C. Audoin, A. Makdissi, P. Laurent, G. Dick, and A. Clairon, Ultrasonics, Ferroelectrics and Frequency Control, IEEE Transactions on **45**, 887 (1998).

[12] E. Peik, T. Schneider, and C. Tamm, J. Phys. B: At. Mol. Opt. Phys. **39**, 145 (2006).

[13] N. Herschbach, K. Pyka, J. Keller, and T. E. Mehlstäubler, Appl. Phys. B **107**, 891 (2012).

[14] K. Pyka, N. Herschbach, J. Keller, and T. E. Mehlstäubler, Appl. Phys. B **114**, 231 (2014).

[15] W. M. Itano, J. Res. NIST **105**, 829 (2000).

[16] H. Dehmelt, Le Journal de Physique Colloques **42**, 299 (1981).

[17] S. Schiller, Phys. Rev. Lett. **98**, 180801 (2007).

[18] A. Derevianko, V. A. Dzuba, and V. V. Flambaum, Phys. Rev. Lett. **109**, 180801 (2012).

[19] V. A. Dzuba, A. Derevianko, and V. V. Flambaum, Phys. Rev. A **86**, 054502 (2012).

[20] V. A. Dzuba, V. V. Flambaum, and H. Katori, arXiv:1411.0775 [physics] (2014), arXiv: 1411.0775.

[21] P. O. Schmidt, T. Rosenband, C. Langer, W. M. Itano, J. C. Bergquist, and D. J. Wineland, Science **309**, 749 (2005).

[22] K. Mølmer and A. Sørensen, Phys. Rev. Lett. **82**, 1835 (1999).

[23] E. Solano, R. L. de Matos Filho, and N. Zagury, Phys. Rev. A **59**, R2539 (1999).

[24] G. Milburn, S. Schneider, and D. James, Fortschritte der Physik **48**, 801 (2000).

[25] C. F. Roos, New Journal of Physics **10**, 013002 (2008).

[26] K.-A. B. Soderberg and C. Monroe, Reports on Progress in Physics **73**, 036401 (2010).

[27] R. Blatt and C. F. Roos, Nat Phys **8**, 277 (2012).

[28] C. H. Bennett, H. J. Bernstein, S. Popescu, and B. Schumacher, Phys. Rev. A **53**, 2046 (1996).

[29] P. Kaye and M. Mosca, Journal of Physics A: Mathematical and General **34**, 6939 (2001).

[30] V. Bužek, R. Derka, and S. Massar, Phys. Rev. Lett. **82**, 2207 (1999).

[31] T. Rosenband, P. Schmidt, D. Hume, W. Itano, T. Fortier, J. Stalnaker, K. Kim, S. Diddams, J. Koelemeij, J. Bergquist, and D. Wineland, Physical Review Letters **98**, 220801 (2007).

[32] G. J. Dick, in *Proc. 19th Annual Precise Time and Time Interval (PTTI) Application and Planning Meeting* (1987) pp. 133–147.

[33] G. J. Dick, J. D. Prestage, J. D. Prestage, and L. Maleki, in *Proc. 22nd Annual Precise Time and Time Interval (PTTI) Applications and Planning Meeting* (1990) pp. 487–508.

[34] Formally, $|N\rangle_{\mathrm{C}} = \binom{N}{N_{\mathrm{C}}}^{-1/2} J_+^N \otimes_{i=1}^{N_{\mathrm{C}}} |0\rangle$ where $J_+ = \sum_{i=1}^{N_{\mathrm{C}}} \sigma_+^i$.

[35] J. P. Home, , 30 (2013), arXiv:1306.5950.

[36] D. Kielpinski, B. King, C. Myatt, C. Sackett, Q. Turchette, W. Itano, C. Monroe, D. Wineland, and W. Zurek, Phys. Rev. A **61**, 032310 (2000).

[37] G. Morigi and H. Walther, The European Physical Journal D **269**, 261 (2001).

[38] D. McGloin, G. Spalding, H. Melville, W. Sibbett, and K. Dholakia, Opt. Express **11**, 158 (2003).

[39] We use Powell's method as implemented in SciPy for the numerical minimization.

[40] M. A. Nielsen and I. L. Chuang, *Quantum Computation and Quantum Information* (Cambridge University Press, 2000).

[41] J. R. Johansson, P. D. Nation, and F. Nori, Computer Physics Communications **183**, 16 (2011), arXiv:1110.0573.

[42] J. Johansson, P. Nation, and F. Nori, Computer Physics Communications **184**, 1234 (2013).

[43] P. A. Barton, C. J. S. Donald, D. M. Lucas, D. A. Stevens, A. M. Steane, and D. N. Stacey, Phys. Rev. A **62**, 032503 (2000).

[44] J. Benhelm, G. Kirchmair, C. F. Roos, and R. Blatt, Nat. Physics **4**, 463 (2008).

Appendix

Calculation of normal mode spectrum for transversal ion oscillations

We calculate the normal mode spectrum for the transversal oscillations of a two-species ion chain along the lines of [37]. In the example setup described in the main text two logic ions (Ca^+, mass $m_L = 40$amu, laser wavelength $\lambda_L = 729.1$nm) and three clock ions (Al^+, mass $m_C = 27$amu, laser wavelength $\lambda_C = 267.4$nm) are trapped along the crystal axis (z-axis). The trap frequency for the logic ions is $\nu_z^L = 2\pi 874$kHz. The asymmetry parameters are defined as $a = \nu_x^L/\nu_z^L$ and $a_{yx} = \nu_y^L/\nu_x^L$. We fix $a_{yx} = 5$ to suppress oscillations along the y-axis. The normal modes are calculated for different values of a, because the oscillations in x-directions will be used for the gate. As sketched in Fig. 3b the clock ions (index $k = 2, 3, 4$) are placed in the middle and the logic ions (index $k = 1$ and $k = 5$) on the outside. With masses $(m_1, m_2, m_3, m_4, m_5) = (m_L, m_C, m_C, m_C, m_L)$ the kinetic energy is given by

$$T(\vec{p}) = \sum_{k=1}^{5} \vec{p}_k^{\,2}/2m_k.$$

The potential energy due to the electrostatic component of the trap is the same for each ion, as all ions carry a single positive elementary charge q. Assuming a radially symmetric electrostatic trap we get a total electrostatic potential of [36]

$$V_S(\vec{x}) = \tfrac{1}{2}\sum_{k=1}^{5}\left(b_0 z_k^2 - \tfrac{1}{2}b_0 x_k^2 - \tfrac{1}{2}b_0 y_k^2\right),$$

i.e.trapping in z-direction but repulsion in x- and y-direction of equal strength. The potential strenth is parametrized by the parameter b_0, in units of energy divided by length squared. To keep the ions also radially trapped, an additional time-dependent radiofrequency potential is used to create an effective mass-dependent potential in x and y direction

$$V_{RF}(\vec{x}) = \tfrac{1}{2}\sum_{k=1}^{5}\frac{m_L}{m_k}\left(b_x x_k^2 + b_y y_k^2\right).$$

The potential strength is parametrized by b_x and b_y, in the same units as b_0. The parameters b_0, b_x and b_y are fully determined by the physical parameters of the setup: logic ion mass m_L, logic ion frequency ν_z^L and the asymmetry parameters a and a_{xy}. In addition to the trapping potential the ions interact via the Coulomb repulsion potential

$$V_I(\vec{x}) = \sum_{k>j}\frac{q^2}{4\pi\epsilon_0}\left|\vec{x}_k - \vec{x}_j\right|^{-1}.$$

With these definitions we can write the total energy of the system as $E(\vec{x},\vec{p}) = T(\vec{p}) + V(\vec{x})$, where $V(\vec{x}) = V_S(\vec{x}) + V_{RF}(\vec{x}) + V_I(\vec{x})$.

We find the steady state position $\vec{x}_0$ of the ions by numerically minimizing [39] the potential energy V under the condition $z_1 < z_2 < ... < z_5$. In this study we choose large enough asymmetry parameters a so that the solution is always a linear chain without zigzag configuration [35–37]. As the oscillations around the steady state will be small, we use second order Taylor expansion to obtain an approximate harmonic potential. The different directions x, y and z decouple in this approximation. Denoting $p_k = m_k\dot{x}_k$ and $V_{kj} = \partial_{x_k x_j}V(\vec{x})\Big|_{\vec{x}_0}$ the energy for motion in x-direction only is

$$E_x = \sum_{k=1}^{5}\frac{p_k^2}{2m_k} + \sum_{k,j}\frac{1}{2}V_{kj}x_k x_j.$$

In coordinates with scaled position $\tilde{x}_k = \sqrt{\frac{m_k}{m_0}}x_k$ and momentum $\tilde{p}_k = \sqrt{\frac{m_0}{m_k}}p_k$, normalized to mass $m_0 = 1$ amu, the kinetic term becomes diagonal and the potential transforms as $\tilde{V}_{kj} = \sqrt{\frac{m_0^2}{m_k m_j}}V_{kj}$. In these coordinates E_x reads

$$E_x = \sum_{k=1}^{5}\frac{\tilde{p}_k^2}{2m_0} + \sum_{k,j}\frac{1}{2}\tilde{V}_{kj}\tilde{x}_k\tilde{x}_j.$$

For the normal modes we numerically diagonalize $\tilde{V} = ODO^T$ with a dimensionless orthogonal matrix O and diagonal matrix D of dimension frequency squared times mass. The eigenfrequencies are then given by

$$\nu_k = \sqrt{D_{kk}/m_0}.$$

In analogy to [37] the Lamb-Dicke factors of a mode k for an individual ion with index j are

$$\eta_j^k = \frac{2\pi}{\lambda_j}O_j^k\sqrt{\frac{\hbar}{2m_j\nu_k}},$$

with λ_j the wavelength of the laser addressing the j-th ion and O_{jk} the j-th entry of the eigenvector for the k-th normal mode.

Derivation of the effective MS-Hamiltonian

A MS-gate is achieved by the interaction of multiple ions with two laser fields equally detuned to the upper and lower sideband of a collective motional mode [22, 25]. The two lasers A and B (red and blue detuned, respectively) have frequencies $\omega_A = \omega_0 - \nu - \delta$ and $\omega_B = \omega_0 + \nu + \delta$ where ω_0 is the carrier frequency, ν is the frequency of the motional mode mediating the interactions and δ is a small detuning of the lasers to the motional sidebands. First we assume a general setup of N arbitrary ions with individual Lamb-Dicke factors $\eta_{A/B,i}$ and Rabi frequencies $\Omega_{A/B,i}$ and laser phase ϕ_i (assumed to be equal for both lasers A and B but possibly different for each ion). The Hamiltonian of the system consists of the internal energies, motional energy and the interaction with the lasers. Changing into an interaction picture gives a time dependent Hamiltonian in Lamb-Dicke expansion

$$\mathcal{H}(t) = \sum_{j=1}^{N} \Omega_{A,j}\eta_{A,j}\left(e^{-i\delta t}e^{-i\phi_j}\sigma_j^+ a + \text{h.c.}\right) + \Omega_{B,j}\eta_{B,j}\left(e^{i\delta t}e^{-i\phi_j}\sigma_j^+ a^\dagger + \text{h.c.}\right).$$

Here $a^\dagger$ and a are the creation and annihilation operators of the joint motional mode with frequency ν. The Lamb-Dicke approximation was used keeping terms only to linear order in $\eta_{A/B,j}$ and a rotating wave approximation was applied, neglecting all terms rotating faster than δ. The laser phases can be absorbed through a unitary transformation $\mathcal{H}(t) = V\tilde{\mathcal{H}}V^\dagger$ where

$$V = \prod_{j=1}^{N} \exp\left(-i\frac{\phi_j}{2}\sigma_j^z\right)$$

such that

$$\tilde{\mathcal{H}}(t) = \sum_{j=1}^{N} \Omega_{A,j}\eta_{A,j}\left(e^{-i\delta t}\sigma_j^+ a + \text{h.c.}\right) + \Omega_{B,j}\eta_{B,j}\left(e^{i\delta t}\sigma_j^+ a^\dagger + \text{h.c.}\right).$$

For the MS-gate the effective Hamiltonian can be calculated from $\tilde{\mathcal{H}}(t)$ with a Dyson-Series

$$\begin{aligned} U(\Delta t) &= \mathcal{T}\ \exp\left(-i\int_0^{\Delta t} dt'\ \tilde{\mathcal{H}}(t')\right) \\ &= \mathbb{1} + (-i)\int_0^{\Delta t} dt'\ \tilde{\mathcal{H}}(t') + (-i)^2\int_0^{\Delta t} dt'\int_0^{t'} dt''\ \tilde{\mathcal{H}}(t')\tilde{\mathcal{H}}(t'') + \dots \end{aligned}$$

Here $\mathcal{T}$ is the time-ordering operator and a rotating wave approximation is applied to derive the time independent effective Hamiltonian. This means neglecting all terms of order $e^{i\delta t}$ or higher powers. Since the first order correction is linear in $\tilde{\mathcal{H}}(t')$ this term will be neglected because every part is proportional to either $e^{i\delta t}$ or $e^{-i\delta t}$. Therefore the first contributions to the effective Hamiltonian are of second order, when rotating and counter rotating terms from $\tilde{\mathcal{H}}(t')$ and $\tilde{\mathcal{H}}(t'')$ cancel. The infinite series can then be summed to give the unitary time evolution of the effective Hamiltonian

$$U(\Delta t) = \exp\left(-i\tilde{\mathcal{H}}_{\text{eff}}\Delta t\right).$$

Up to a constant, $\tilde{\mathcal{H}}_{\text{eff}}$ can be written in a compact form as

$$\tilde{\mathcal{H}}_{\text{eff}} = \frac{1}{4\delta}\left[\tilde{S}_x^2 + \tilde{S}_y^2 + \tilde{S}_z\right]$$

where

$$\begin{aligned} \tilde{S}_x &= \sum_{j=1}^{N}\left(\Omega_{A,j}\eta_{A,j} + \Omega_{B,j}\eta_{B,j}\right)\sigma_j^x, \\ \tilde{S}_y &= \sum_{j=1}^{N}\left(\Omega_{A,j}\eta_{A,j} - \Omega_{B,j}\eta_{B,j}\right)\sigma_j^y \\ \tilde{S}_z &= \sum_{j=1}^{N} 2\left(\Omega_{A,j}\eta_{A,j} + \Omega_{B,j}\eta_{B,j}\right)\left(\Omega_{A,j}\eta_{A,j} - \Omega_{B,j}\eta_{B,j}\right)\left(2a^\dagger a + 1\right)\sigma_j^z \end{aligned}$$

This representation emphasizes the different contributions to the effective Hamiltonian. $\tilde{S}_x^2$ and $\tilde{S}_y^2$ give rise to the usual collective spin flips in a MS-gate and S_z are energy shifts for the internal states of the ions. Note that both $\tilde{S}_y$ and $\tilde{S}_z$ are proportional to the differences in Rabi frequencies and Lamb-Dicke factors for the lasers A or B and therefore vanish if those are equal.

Now the unitary transformation, with V given above, is applied to $\tilde{\mathcal{H}}_{\text{eff}}$ to find the full Hamiltonian of the MS interaction, namely

$$\mathcal{H}_{\text{MS}} = V\tilde{\mathcal{H}}_{\text{eff}}V^\dagger = \frac{1}{4\delta}\left[\left(\tilde{S}_x^\phi\right)^2 + \left(\tilde{S}_y^\phi\right)^2 + \tilde{S}_z\right]$$

with the operators

$$\tilde{S}_x^\phi = \sum_{j=1}^{N}\left(\Omega_{A,j}\eta_{A,j} + \Omega_{B,j}\eta_{B,j}\right)\left(\sigma_j^x \cos\phi_j - \sigma_j^y \sin\phi_j\right)$$
$$\tilde{S}_y^\phi = \sum_{j=1}^{N}\left(\Omega_{A,j}\eta_{A,j} - \Omega_{B,j}\eta_{B,j}\right)\left(\sigma_j^y \cos\phi_j + \sigma_j^x \sin\phi_j\right)$$

and $\tilde{S}_z$ stays unchanged.

If we assume now that each ion interacts with both laser beams in the same way, meaning that $\Omega_{A,j} = \Omega_{B,j} \equiv \Omega_j$ and $\eta_{A,j} = \eta_{B,j} \equiv \eta_j$ hold for each ion j, the Hamiltonian reduces to only one term.

$$\mathcal{H}_{\text{MS}} = \frac{\Omega_j^2\eta_j^2}{\delta}\left(\sum_{j=1}^{N}\sigma_j^x \cos\phi_j - \sigma_j^y \sin\phi_j\right) \otimes \left(\sum_{k=1}^{N}\sigma_k^x \cos\phi_k - \sigma_k^y \sin\phi_k\right)$$

Finally, to compare this result to the quantum gate used in the main text, we calculate the unitary time evolution for this Hamiltonian.

$$U_{\text{MS}} = \exp\left(-i\mathcal{H}_{\text{MS}}\, t\right) = \exp\left(-iS^2\right)$$

where t is the gate time and

$$S = \sum_{j=1}^{N}\Omega_j\eta_j\sqrt{t/\delta}\left(\sigma_j^x \cos\phi_j - \sigma_j^y \sin\phi_j\right)$$

This is identical to the unitary evolution used in the readout strategy if we label the N ions accordingly as clock or logic-ions, i.e $j \to \alpha i$.

Generalised Algorithmic Readout

So far the readout algorithm was discussed only for $N_{\text{C}} = 3$, $N_{\text{L}} = 2$. This section describes the case with arbitrary N_{C} and N_{L} and gives an explicit description of all quantum gates used to implement the algorithm. The generalisation of the schematic circuit in Fig. 2a to the case of arbitrary numbers of ions is shown in Fig. 4a. The Ramsey-sequence is performed on all clock ions (leaving them in a superposition of states $|N\rangle_{\text{C}}$), and the logic ions are prepared in the ground state at the beginning of the algorithm $\mathcal{U}$. After applying the quantum fourier transformation on the logic ions the algorithm consists of controlled phase gates using the clock ions as control bits. This way an excited clock ion gives an additional phase to the excited state in each logic ion via the unitary phase gate $R_k = \begin{pmatrix} 1 & 0 \\ 0 & e^{2\pi i/2^k} \end{pmatrix}$ and generates the state $|N\rangle_{\text{C}}|\underline{\mathbf{N}}\rangle_{\text{L}}$. The inverse quantum fourier transformation produces the Hamming-weight N in binary representation as the logic ions' state, which can then be retrieved by a measurement on the logic ions.

Generalising the implementation of the readout by means of MS gates requires some more work than the schematic description, mostly due to the inverse quantum fourier transformation. The initial quantum fourier transformation in $\mathcal{U}$ is again given by Hadamard gates on the logic ions, since they were initially prepared in the ground state. The

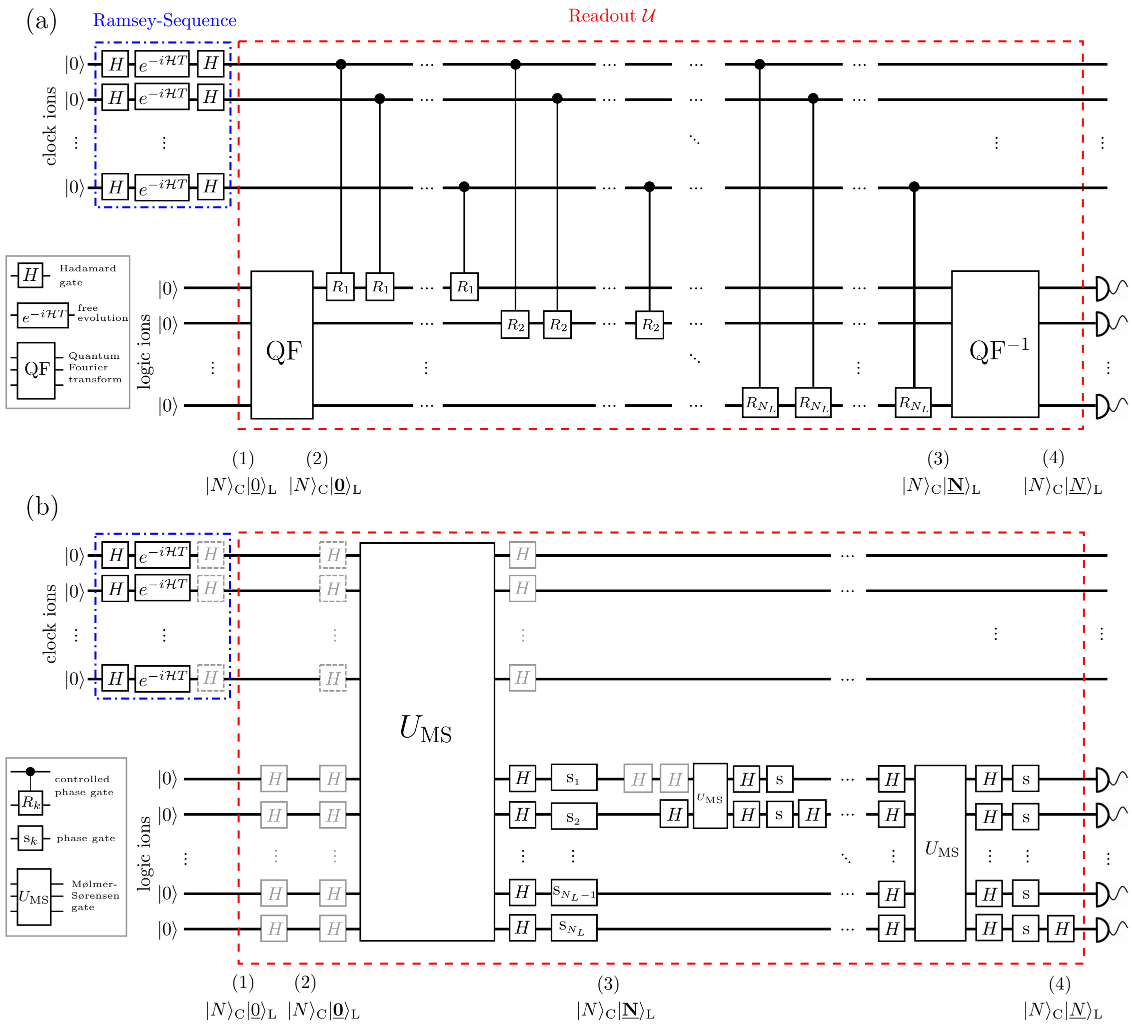

FIG. 4. Full algorithmic Readout for a general number of clock- and logic ions N_{C},N_{L}. (a) As described in the main text, the clock cycle starts with a Ramsey sequence (blue, dash-dotted box) on all N_{C} clock ions, uses the quantum algorithm $\mathcal{U}$ (red, dashed box) to encode the number of excited clock ions onto the N_{L} logic ions and gives Hamming weight in binomial representation with a subsequent measurement of each logic ion. So the unitary transformation $\mathcal{U}$ starts at (1) with the state $|N\rangle_{\mathrm{C}}|\underline{0}\rangle_{\mathrm{L}}$ where N clock ions are in the excited state and all logic ions are prepared in the ground state. Then the quantum fourier transform is applied to the logic ions to give $|N\rangle_{\mathrm{C}}|\mathbf{0}\rangle_{\mathrm{L}}$ as the resulting state at (2). The controlled phase gates R_k add additional phases to the logic ions for each excited clock ion to give the state $|N\rangle_{\mathrm{C}}|\mathbf{N}\rangle_{\mathrm{L}}$ at (3). The inverse quantum fourier transform yields the state $|N\rangle_{\mathrm{C}}|\underline{N}\rangle_{\mathrm{L}}$ at (4) so that the detection of each logic ion gives the binary representation of N. (b) Decomposition into quantum gates for an experimental realisation. In the first step the quantum fourier transformation is performed via Hadamard gates on the logic ions. Then a Mølmer-Sørensen-gate connecting clock- and logic ions transfers the information about the Hamming weight onto the logic ions. The inverse quantum fourier transformation is decomposed into $N_{\mathrm{L}}-1$ Mølmer-Sørensen-gates and related single ion phase gates separated by a Hadamard gate. For simplicity each phase gate is labeled s although they all describe different phase shifts. The detailed phases for s and the coefficients for each U_{MS} operation are given in the text. Again, Hadamard gates shown in grey drop in pairs and do not need to be executed. Grey dashed gates merge the readout with the Ramsey sequence.

main part of the algorithm, i.e. the controlled phase gates between clock- and logic ions, are performed by a single Mølmer-Sørensen gate and additional single qbit phase gates. This Mølmer-Sørensen gate is described in the main text and Eq. (5) shows the coefficients needed to implement the desired algorithm. In Fig. 4b the single phase gates associated with this U_{MS} are labeled as s_k. Those are controlled phase gates

$$s_k = \begin{pmatrix} 1 & 0 \\ 0 & e^{i\theta_k} \end{pmatrix} \tag{6}$$

with phases $\theta_k = 2N_{\mathrm{C}}\ \pi\ 2^{-(k+2)}$ for $k = 1, ..., N_{\mathrm{L}}$. Additional single ion phase gates (and Hadamard gates) on the clock ions are left out in this discussion as well as in the given figures (displayed in grey). These gates are only necessary to recover the initial state of the clock ions, but this is not the focus of the algorithmic readout presented here. Hadamard transformations surrounding the Mølmer-Sørensen gates are used to relate the physical $\sigma_x \otimes \sigma_x$ to $\sigma_z \otimes \sigma_z$.

With more logic ions, the implementation of the inverse quantum fourier transformation become more costly in terms of the Mølmer-Sørensen-gates needed. An efficient circuit for the quantum fourier transformation consists of blocks with different controlled phase gates separated by Hadamard gates, see e.g. [40]. In analogy to other parts of the readout, these steps are performed using Mølmer-Sørensen-gates and single ion phase gates. The inverse quantum fourier transformation on the logic ions is implemented by a series of $N_\mathrm{L} - 1$ such steps, each involving an increasing number of ions and ending with a Hadamard gate on the last ion involved. Every Mølmer-Sørensen gate is described by the same mechanism as given by Eq. (1) in the main text but with phases e.g. $\phi_{Lj} = 0$ for all j. It is therefore determined by the coefficients d_j corresponding to the j-th logic ion. For the step involving logic ions 1 to k the coefficients are

$$d_j = \sqrt{2\pi} \cdot 2^{j-2}$$

for $j = 1, 2, ..., k-1$ and

$$d_k = \sqrt{2\pi} \cdot 2^{-k}$$

for ion k. For $k = N_\mathrm{L}$ and $j = N_\mathrm{L} - 1$ the coefficient $d_{N_\mathrm{L}-1} = \sqrt{2\pi} \cdot 2^{N_\mathrm{L}-3}$ gives the extreme case, requiring the largest Rabi frequencies. This sets a limit to possible implementations of this algorithm for large N_L. The corresponding single ion phase gate for ion n in this step are therefore given by Eq. (6) with

$$\theta_j = 2\pi \cdot 2^{-(k-j)}$$

for $j = 1, 2, ..., k-1$ and

$$\theta_k = 2\pi \sum_{m=1}^{k-1} 2^{-(k-m)}$$

for the k-th ion. These coefficients are chosen such that they give the desired controlled phase gates and also discard undesired interactions among the logic ions.

Numerical Simulation of Noise Added in Readout

We denote the excitation probability of each ion after the Ramsey sequence by p. The quality of the clock is characterized (among other parameters such as the readout time) by the derivative of the mean signal $\partial_p \langle \hat{N}_\mathrm{est} \rangle$ and the variance $\sigma^2_\mathrm{est} = \langle \hat{N}^2_\mathrm{est} \rangle - \langle \hat{N}_\mathrm{est} \rangle^2$ of the number of excitations $\hat{N}_\mathrm{est}$. The values are taken at a detuning where $p = 0.5$, as the clock is operated around that point for best results. For the ideal case of perfectly noiseless ion gates, $\hat{N}_\mathrm{est}$ follows the same statistics as $\hat{N}$ before readout with variance $\sigma^2 = \langle \hat{N}^2 \rangle - \langle \hat{N} \rangle^2$. Any indirect readout will add additional decoherence which decreases the signal and increases the variance. We define the readout quality $\zeta \leq 1$ as the quotient

$$\zeta = \left. \frac{\partial_p \langle \hat{N}_\mathrm{est} \rangle / \sigma_\mathrm{est}}{\partial_p \langle \hat{N} \rangle / \sigma} \right|_{p=0.5}$$

of the physical signal to noise ratio (SNR) and the ideal SNR.

Here we consider in particular noise sources due to spontaneous decay of the ions (mostly the logic ions) as well as additional phase noise of the logic ions, due to e.g. stray magnetic fields. The execution of the five-ion MS gate defined just before Eq. (1) consumes by far the most time ($T = 1$ms for our parameters) of the readout process, as its speed is limited by the restrictions on the Rabi frequency described in the main text. We thus simulate only these two noise sources and only while executing the five-ion MS gate.

The numerics is implemented using the master equation solver from QuTiP [41, 42]. The Hamiltonian for the gate operation is given by $H_\mathrm{MS} = S^2/T$ with S from Eq. (1). Note that our numerical model operates on the qubit level and does not include possible decoherence due to excitations of other phonon modes. Defining for a given operator x

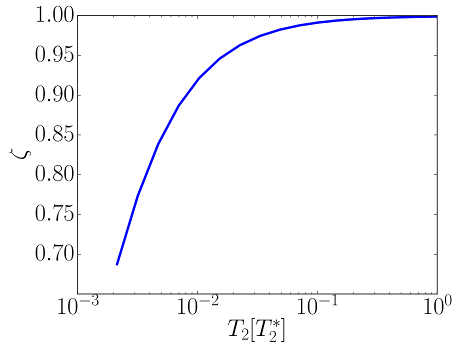

FIG. 5. Plot of ζ for a gate time of 1ms. $T_2^* = 2T_1 = 2.34$ s is the maximal possible value of T_2 for the logic ions considering their finite lifetime due to spontaneous emission.

a corresponding superoperator $D[x]\rho = x\rho x^\dagger - \frac{1}{2}x^\dagger x\rho - \frac{1}{2}\rho x^\dagger x$ acting on a density matrix ρ, the Lindblad operator for the spontaneous emission (index SE) of the j-th ion with lifetime τ_j is $L_{\mathrm{SE}}^{(j)} = \frac{1}{\tau_j}D[\sigma_-^{(j)}]$, where σ_- is the lowering operator. In total $L_{\mathrm{SE}} = \sum_j L_{\mathrm{SE}}^{(j)}$. The lifetime of the $D_{5/2}$ state in Ca^+ is $\tau_L = 1.17$ s [43] and the lifetime of the ${}^3P_0$ clock state of Al^+ is $\tau_C = 20.6$ s [31]. The dephasing due to other sources is characterized by a decay rate γ for all ions and the corresponding Lindblad operator is $L_B = \sum_j \gamma D[\sigma_z^{(j)}]$. The full master equation now reads $\dot{\rho} = -i[H,\rho] + L_{\mathrm{SE}}\rho + L_B\rho$. While the T_1 coherence time of the logic ions is fixed, $T_1 = \tau_L$, the T_2 coherence time also depends on the experiment-dependent (phenomenological) decay rate γ via $T_2 = 1/(0.5\tau_L^{-1} + 2\gamma)$. The numerical result for ζ as a function of T_2 is depicted in Fig. 5. The best achievable value, reached at $T_2^* = 2T_1$, is $\zeta(T_2^*) = 0.999$ for a gate time of 1ms.

Note that, in general terms, the concentration of information from N_{C} clock ions into $N_{\mathrm{L}} \sim \lceil \log_2 N_{\mathrm{C}} \rceil$ logical ions entails an increase in the cost of certain errors. For instance, an error in the most significant bit in the binary representation $|\underline{N}\rangle_L = |i_1 i_2 \ldots i_{N_{\mathrm{L}}}\rangle_{\mathrm{L}}$ is equivalent to an error on the count N of $N_{\mathrm{C}}/2$. This is acceptable as long as the noise added by such errors is smaller than the unavoidable quantum projection noise in the readout of N_{C} clock ions. This implies $\epsilon \ll 3/4N_{\mathrm{C}}$, where ϵ is the single-qubit error rate. Mølmer-Sørensen gate fidelities sufficient to satisfy this criterion for clock operation with dozens of ions have already been demonstrated [44].